10º Congreso de Exploración y Desarrollo de Hidrocarburos
Sesiones Generales: "Energía y Sociedad, aliados inseparables"

ALLUVIAL ARCHITECTURE AND FLUVIAL STYLE VARIATIONS DETERMINED FROM OUTCROPS: EXAMPLE FROM THE CERRO BALLENA ANTICLINE (BAJO BARREAL FORMATION) OF THE GOLFO SAN JORGE BASIN

José Matildo Paredes[1], Nicolás Foix[1,2], José Oscar Allard[1], Mauro Nicolás Valle[1,2], Sergio Roberto Giordano[3]

1: Universidad Nacional de la Patagonia San Juan Bosco, paredesjose@yahoo.com, joseoallard@yahoo.com.ar

2: CONICET, nicofoix@hotmail.com, mauro_09_valle@hotmail.com

3: Sinopec Argentina E&P Inc, sergio_giordano@sinopecarg.com.ar

Keywords: **alluvial architecture, multichannel fluvial system, incisional avulsion, Upper Cretaceous, Golfo San Jorge Basin**

RESUMEN

Arquitectura fluvial y variaciones en los estilos fluviales determinados en afloramientos: el ejemplo del anticlinal del Cerro Ballena (Formación Bajo Barreal) de la cuenca del Golfo San Jorge.
Se realizó un estudio sedimentológico y de arquitectura fluvial en una sucesión de 380 m de potencia de la Formación Bajo Barreal (Cretácico Superior) en el anticlinal del cerro Ballena, provincia de Santa Cruz. Los afloramientos estudiados muestran, en la base, fajas de canales aisladas de pequeña escala en una planicie de inundación silicoclástica. La sucesión cambia verticalmente a fajas de canales multiepisódicas de gran escala y mayor interconectividad dentro de una planicie de inundación volcaniclástica. La sucesión contiene diecisiete litofacies y doce elementos arquitecturales, que brindan información sobre la organización aluvial de depósitos de canal y de planicie de inundación. Se identificaron cinco tipos de fajas de canales: multiepisódicas dominadas por acreción frontal (90%), mantos con acreción lateral (5%), fajas de canales rellenas con materiales volcaniclásticos resedimentados (3%), mantos multilaterales dominados por acreción frontal (1%) y canales fijos con geometría en cinta (1%). Los datos de paleoflujo obtenidos en 218 canales fluviales (Az. 187º; n= 3777) indican la presencia de un depocentro localizado hacia el sur del río Deseado, mientras que la geometría y estilos variables de los paleo-cauces dispuestos en niveles lateralmente equivalentes, y el predominio de mecanismos avulsivos indican que el sistema fluvial fue multicanalizado (anastomosado o anabranching). Se destaca que en las zonas con mayor interconectividad los canales fluviales tienen mayor potencia y ancho real, que se relaciona al desarrollo de canales fluviales de mayor descarga. Aunque algunas fajas de canales tienen buen desarrollo de acreción lateral, la mayoría de los canales migraron por procesos avulsivos, identificando los tres tipos conocidos de avulsión. La incisión avulsional es el mecanismo dominante de migración de las fajas de canales, identificado por la relocalización súbita de la faja de canales sobre materiales de grano fino depositados en la planicie distal, sin preservación de sucesiones granocrecientes de escala métrica de planicie de inundación proximal. En otros casos, ocurrió avulsión por progradación de la faja de canal sobre la planicie de inundación proximal, y en pocos casos se observó la re-ocupación de fajas de canales previamente abandonadas. Los resultados de este estudio colaboran en el entendimiento de la organización espacio-temporal del sistema fluvial, los tipos de canales y sus geometrías, con implicancias para la explotación de hidrocarburos en la cuenca del Golfo San Jorge.

INTRODUCTION

The architecture and evolution of fluvial systems has been of particular interest in both the hydrocarbon industry and academic study in recent years, with detailed investigations using high-resolution 3-D seismic surveys (Posamentier *et al.* 2007; El-Mowafy and Mardfur 2016) modelling studies (Hajek and Wolinsky 2012; Keogh *et al.* 2014) and field-based studies (Hampson *et al.* 2013; Allen *et al.* 2014; Ghinassi *et al.* 2016, among others). As three-dimensional seismic data does not allow to detect bed-scale stratigraphic and sedimentary discontinuities in cross-sections, the use of analogous systems at outcrops help to constrain the distribution and lateral variation of sedimentary facies of channel fills, channel-scale stacking styles and stratigraphical relationship with adjacent floodplain facies (Rittersbacher *et al.* 2014; Pranter *et al.* 2014; Paredes *et al.* 2016).

The Golfo San Jorge Basin, which is located in Central Patagonia, is a prolific hydrocarbon province with about 10 billion barrels of oil (1,500 million m^3) produced in more than 100 years, currently providing 48.8% of the of the country oil production and 12.7% of gas (Secretaría de Energía 2016). Up to 90% of the basin hydrocarbons are recovered from fluvial channels in the

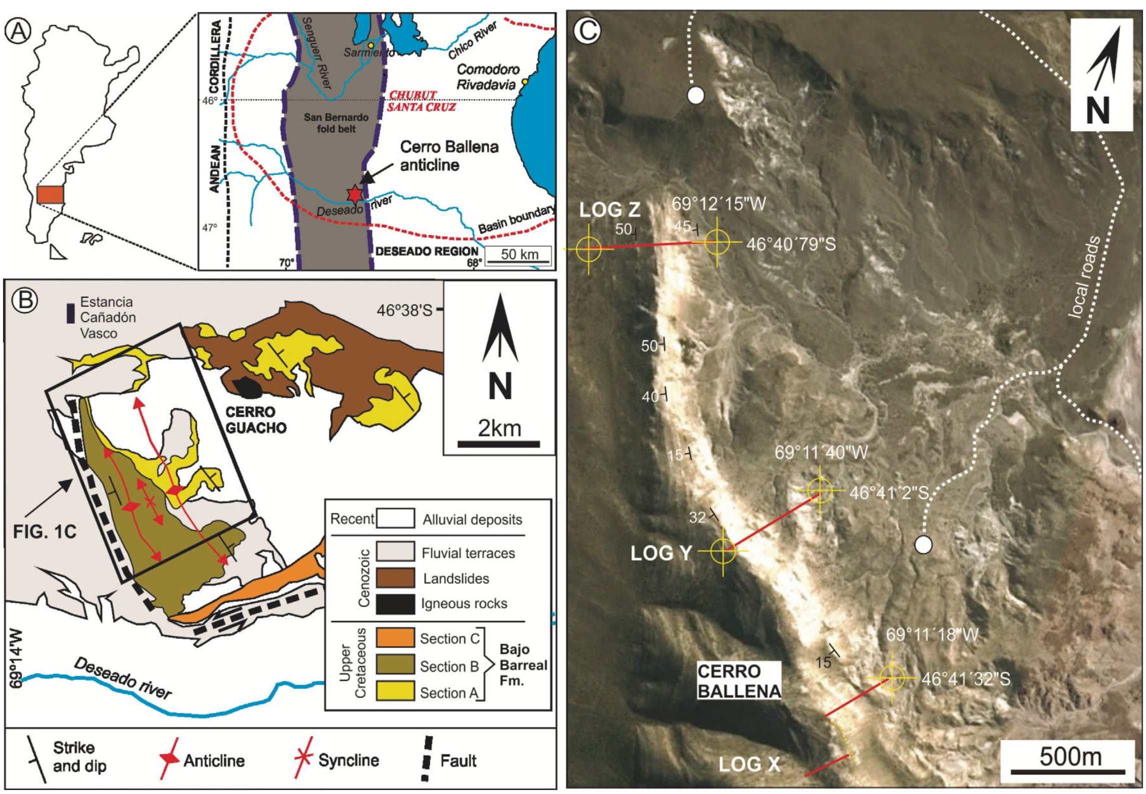

Figure 1. Location map of the Golfo San Jorge Basin in central Patagonia, Argentina, with the location of the Cerro Ballena anticline (star). (B) Simplified geological map of the area of the Cerro Ballena anticline, southwestern Golfo San Jorge Basin (after Figari *et al.* 1998). (C) GoogleTM image of the Cerro Ballena anticline, with location of the sedimentary logs (Logs X, Y and Z). Local roads are indicated with dotted lines.

Upper Cretaceous Bajo Barreal Formation and subsurface equivalents. In addition, the Golfo San Jorge basin holds 2/3 of Argentina's oil reserves. The Bajo Barreal Formation in the Cerro Ballena anticline is a well-known outcrop analogue for fluvial reservoirs that are exposed in excellent sections along a 2500 m width belt (Fig. 1). The Cerro Ballena is a whaleback-shaped anticline, elongated north-south, 5 km long and 1 to 2 km width. It constitutes the western limb of a faulted, plunging anticline, trending NNW-SSE. The Cerro Ballena is bounded to the west by a reverse fault and to the south by the Deseado River. The strike of the strata is N110ºE to N130ºE, and dips range from 3° to 50º.

The aim of this study is to provide an interpretation of the non-marine sedimentation in the Cerro Ballena anticline, for identifying spatial and temporal variations in the alluvial organization of the Bajo Barreal Formation. The specific objectives of this study are: (1) to analyze the alluvial sedimentology and architecture of the two lithological sections exposed in the Cerro Ballena area, (2) to quantify the dimensions (true width/thickness) of fluvial channels or channel belts of both sections, (3) to unravel the first-order control on the alluvial architecture.

Previous research

Previous studies have identified a siliciclastic section with isolated channels at the base (Section A, 180 m thick sensu Figari *et al.* 1998) covered by densely stacked channel belts encased in a fine-grained volcaniclastic floodplain (Section B, 270 m thick sensu Figari *et al.* 1998). Bridge *et al.* (2000) presented a detailed research in the Cerro Ballena anticline, and constitute the foundation of the present study. Bridge *et al.* (2000) took photos and then constructed photomosaics analyzing the internal geometry and organization of the main channel belts; the width and apparent thickness of the sandstones bodies were measured from the tracing (Bridge *et al.* 2000, p. 341). Several detailed sedimentological logs were carried out at selected accessible locations and in selected channel belts. Bridge *et al.* (2000) found that the mean thickness of channel sandbodies ranges from decimeters to up to 6 m (n=117), with true width ranging from 45 to 274m, and a width/thickness ratio from 17 to 53. Bankfull channel depths ranged from 3m to 6m, with reconstructed widths from 35m to 65m. Main paleoflow data of the sandbodies is N82ºE (n=97), with most of the values in the range of N60ºE to N150ºE. A radimetrical age of a distinctive marker bed at the base of Section B, interpreted by Bridge *et al.* (2000) as an ignimbrite, provided an age of 91+/- 0.49 Ma. Most of the fluvial sandbodies are interpreted by Bridge *et al.* (2000) as single channel rivers of relatively low-sinuosity, with ocassional braided rivers and with major spatial changes in sandstone-body proportion and thickness along the exposure.

Methodology

The sedimentary facies of the fluvial succession have been studied by logging at scale 1:50 along well-exposed cliff faces. Seventeen lithofacies and twelve architectural elements were described and interpreted. Approximately 3777 paleocurrent measures, derived from several varieties of cross-bedding sets, supplement the lithofacies information and aid in the reconstruction of the paleogeographic setting. Paleocurrents were corrected according to the geometrical methods (Ramsay 1961). The depositional architecture of the channel belts has been studied in 2D photo mosaics by measuring local bedding attitude of large-scale inclined surfaces, paleoflow data and thickness of cross bedding sets. Two hundred eighteen fluvial sandstone bodies were precisely measured (thickness, width) using the Jacob staff and a global positioning system (GPS). To stratigraphically locate the channels, we measure the floodplain thickness between consecutive fluvial channels, and plotting the coordenates of the extremes of the sandbodies in a fully 2D scenario. The true width of individual or multi-storey channels were measured using GPS point data at their margins, and correcting their apparent width using the mean of the paleocurrent data for each channel. The real width/thickness ratio of fluvial channels (hereafter abbreviated as W:T) was obtained and plotted on frequency histograms and crossplots. Geometry of fluvial channels were classified as ribbons ($W:T < 15$), narrow sheets ($15 > W:T < 100$) and broad sheets ($W:T > 100$) following Gibling (2006) criteria. Our architectural study follows model cross-section diagrams of bars provided by Miall (1985, 1996) and Bridge (1993, 2003).

Sedimentary facies

Detailed descriptions and interpretations of seventeen lithofacies were defined based on their lithology, grain size, sedimentary structures, geometries and boundaries. A selected sedimentological log (Log Y) build up during the field study is presented in Fig. 2. A brief summary of their main attributes, flow properties and facies interpretation are presented in Table I. Most of these facies are common in fluvial deposits (and are therefore not described in detail here); an unusual feature of the analized sections is the abundance of rippled sandstones (Facies Sr), uncommon in most of the exposures of the Bajo Barreal Formation along the San Bernardo Fold Belt (Paredes *et al.* 2016).

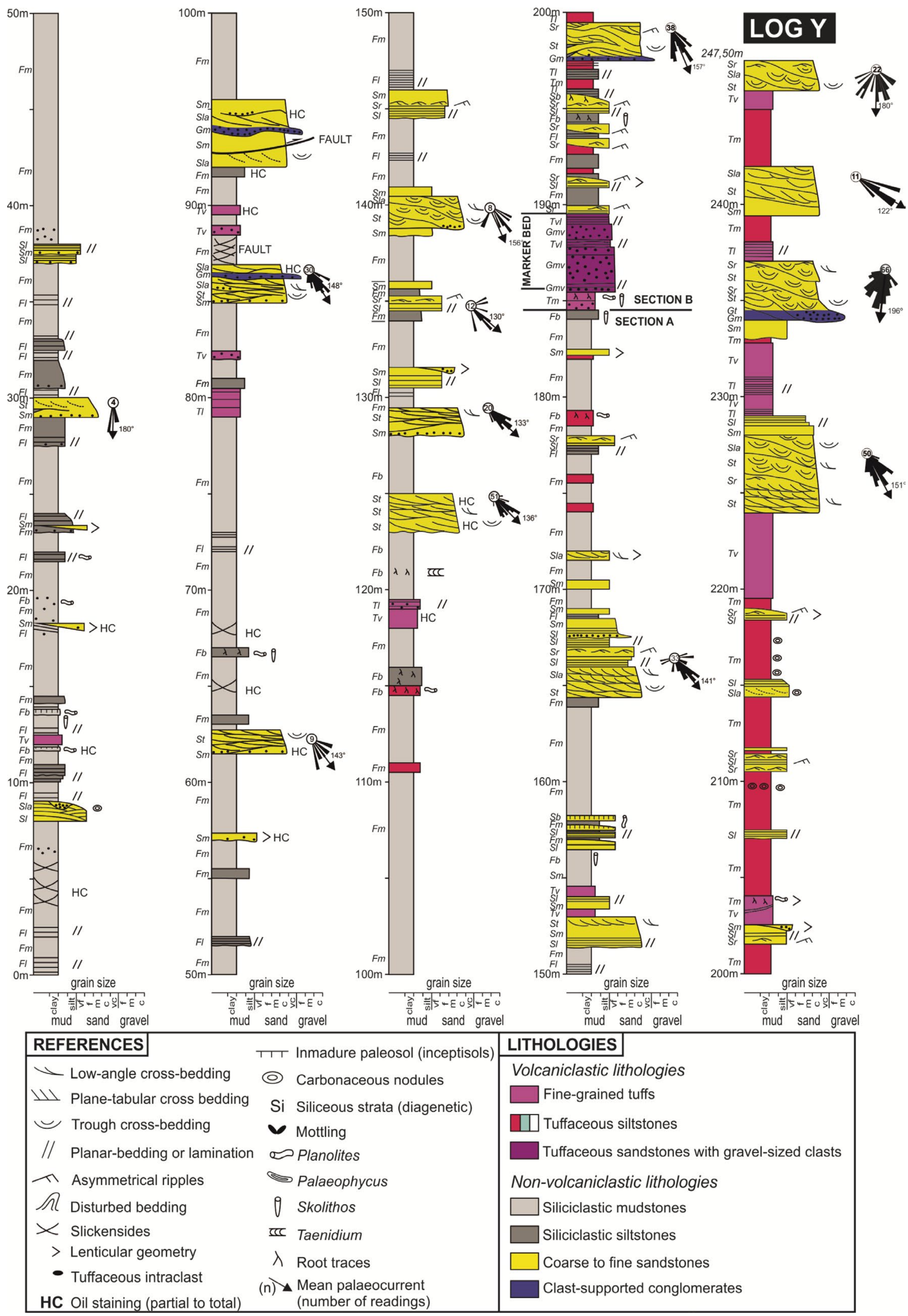

Figure 2. Composite graphic log (Log Y) of the western limb in Cerro Ballena anticline with paleocurrent measurements. Location of the section in Fig. 1C.

Facies and Description	Interpretation
(Gmv) *Massive, matrix supported tuffaceous conglomerate.* Sheet-like strata are up to 1 m thick and have planar or slightly erosive base, and bimodal grainsize. Could contain outsized clasts up to 10 cm in size. Ungraded throughout the bed or coarse-tail normally graded at upper part. Poor quality as reservoir rock.	Volcaniclastic debris flow or mudflow. Bulking from initial turbulent flow and rapid deposition from suspension.
(Gmi) *Massive, clast-supported tuffaceous conglomerate.* Poorly sorted, granule to small pebble tuffaceous conglomerate. Diffuse, horizontal stratification. Poor quality as reservoir rock. Could contain HC staining of medium-grained sandstones. Moderate quality as reservoir rock.	Fluvial channel lag.
(Gt) *Through cross-bedded tuffaceous conglomerate.* Abundant. Tuffaceuos, fine-grained conglomerates with clast or matrix supported texture. Crudely bedded or with trough cross-bedding. Mean size up to 0.5 cm, with rounded clasts up to 7 cm in diameter. Moderate quality as reservoir rock.	Downstream migration of bars or migration of 3D dunes inside channels.
(Sla) *Low-angle cross-bedded sandstone.* Abundant. Slightly erosive base, moderate grain size selection, occasionally with fining upward trend from coarse to fine sandstones. Foresets dip less than 10º. Individual laminae show plane-parallel lamination. Could contain trunk remains. Occasional convolute bedding. Moderate quality as reservoir rock.	Downstream accretion of low relief bedforms with high wavelength/amplitude ratio.
***(St** and **Sp)** Trough (St) and planar (Sp) cross-bedded sandstone.* Fx common, Fp subordinate. Very coarse-grained to fine-grained, sub-angular to sub-rounded clasts showing moderate sorting. Beds average 0.3 to 0.6 m thick, with bedset up to 2 m. Could contain trunk remains or broken dinosaur bones. Good quality as reservoir rock.	Migration of straight-crested or curved-crested bedforms in lower flow regime conditions.
(Sl) *Parallel-laminated sandstone.* Abundant. Medium to very-fine grained sandstones, with planar base and moderate sorting, occasional outsized clasts. Laminae are few mm to 1 cm thick and show normal grading. Frequently interbedded with low-angle cross-bedding and/or massive sandstones. Locally convolute lamination chaotically folded. Moderate to good quality as reservoir rock.	Deposition under upper-flow regime within a fluvial channel, or as an unconfined fluvial sheetflood.
(Sb) *Burrowed sandstone.* Common. Medium to fine-grained sandstones with gradational base to other coarse-grained facies. Contain roots, mottling and several fossil traces, included *Skolithos* sp, *Planolites*, and *Taenidium* sp. Poor quality as reservoir rock.	Destruction of structure due to bioturbation.
(Sm) *Massive sandstone*. Subordinate. Very coarse to very fine, ungraded, structureless sandstones. Strata are tens of cm thick, with scours at base. Interbedded with plane-laminated or trough cross-bedded layers. Poor quality as reservoir rock.	Rapid deposition of bedload during high-discharge conditions.
(Sr) *Current-ripple laminated sandstone.* Abundant. Well sorted, very fine to fine-grained sandstones. Associated to several current-dominated sandstone facies or interbedded with fine-grained, massive tuffaceous material. Strata are less than 20 cm in thickness. Unimodal paleocurrents. Good quality as reservoir rock.	Migration of small bedforms within a fluvial channel or via unconfined flows under lower flow regimes.
***(Fm** and **Fl)** Massive (Fm) or horizontally laminated (Fl) siltstone/ mudstone.* Abundant in the Section A. Pale-grey siltstone with lower amount of mudstone. Where preserved, laminations are less than 5 mm thick. Frequent incorporation of isolated, tuffaceous clast until 1 cm in diameter or small, unorganized wood (carbonaceous) fragments. Could contain slickensides. Seal of potential reservoirs.	Deposition from suspension within a fluvial channel or in a floodplain environment.
***(Fb** and **Tb)** Burrowed mudstone (Fb) or Burrowed tuffaceous siltstone (Tb)*. Strata few cm to tens of centimeters thick with motting, *Skolithos* and unidentified fossil traces. Seal of potential reservoirs.	Settling from suspension and posterior intense bioturbation
***(Tm** and **Tl)** Massive (Tm) or horizontally laminated (Tl), fine-grained tuffaceous sediment*. Abundant in the Section B, rare in the Section A. Laminae are ungraded, but can be normally graded. Contain clasts of coarse tuffaceous sandstones, or pumice fragments up to 1 cm in diameter. Packages can reach up to 10 m of thickness. Contain rootlets, intense mottling and several fossil traces. Some beds contain symmetrical ripples and wood fragments on bedding surfaces. Poor quality as reservoir rock.	Reworking of primary ash-fall beds by aqueous flows. Later pedogenesis of reworked tuffs.
(Tv) *Vitric tuffs.* Strata with planar base and mantle bedding, thickness from few cm to several tens of cm. Could contain pumice outsized clasts interbedded and inverse grading. Biotite grains are commonly oriented parallel lo the laminae. Could de silicified. Seal of potential reservoirs.	Setting of suspended ash in standing water. Subsequent silicification during diagenesis.

Table I. Lihofacies of the Bajo Barreal Formation in Cerro Ballena anticline

Architectural elements (Allen 1983; Miall 1985, 1996) are depositional features contributing to the internal architecture of sand bodies and are the product of dune and bar aggradation or channel fill. The vertical and lateral relationships between the facies in the Cerro Ballena anticline have been used to establish twelve architectural elements (Table II).

Code, Name and facies composition	External/Internal architecture	Interpretation
Channel element (5th order)		
(CH) *Channel.* Any assemblage of Sp, St, Sl, Sr. Gt or Gm typically at base of unit. May include SB, LA, DA, HO and ES elements. Upward fining trend in grain size, and internal scour surfaces. Common fossil traces at top.	Flat or erosional base with concave-up margins to element. Upper surface may be gradational into overbank elements.	Channel with preserved cutbanks
Whithin channel elements (4th order)		
(DA) *Simple downstream accretion elements.* Common. Stacked St cosets, Gm at bases, Sl common. May be capped by Sr sets.	Tabular external form or with convex-up top. Contains accretion surfaces dipping in same direction as St crossbed dip.	Downstream-accretion deposit
(CDA) *Complex downstream accretion.* Dominant. Stacked St cosets, Gm at bases, Sl common, may be capped by Sr sets. 3rd order reactivation surfaces (ES element) characterized by *Skolithos* and *Palaeophycus* ichnogenera. Upward decrease in set thickness.	Paleoflow data are at low angle in relation to dip direction of the accretion surfaces. Convex-up top surfaces defining sigmoidal packages.	Stacked downstream-accretion packages. Variable discharge during deposition.
(LA) *Lateral accretion element.* Ocassional. Stacked St cosets, Gm at bases, Sl common. May be capped by Sr sets. Individual convex-upward packages are about 15-20 m wide and up to 4.2 m thick.	Three to five laterally accreted packages with tabular external form or convex-up top. Contains accretion surfaces with dip directions at high angle to orientation of St trough axes	Lateral-accretion deposit
(LS) *Laminated sheet sandstones.* Facies Sl, gradationally capped by minor St, Sp, and Sr. Thickness of 0.3-0.6 m and meters to tens of meters of apparent width.	Sheet-like, upward-fining units of laminated sandstone, overlying flat to low-relief erosion surface.	Sand accumulation under upper-plane-bed conditions within channels
(HO) Hollow element. Single Sl coset dipping obliquely across or down the centre of the unit	Scoop-shaped erosional base.	Formation and fill of erosional hollow formed at channel confluence
(SB) *Sandy bedforms.* Common. Trough and ripple (St and Sr) assemblage, minor Sla.	Tabular sets, cosets and bounding surfaces in packages up to 2.5 m thick. Rhythmically spaced reactivation surfaces.	Vertical accretion and downstream migration of dune and plane bed deposits.
(ES) *Erosional scour fill.* A lag of tuffaceous intraclasts capped by Gm, St, Sl or Sr facies.	Discontinuous sandbody within concave-upward erosional scour situated in channel fill (element CH).	Scour fills developed on channel floor and tops and flanks of bars
(FFC) Interbedded Sr, Sm and Fm facies, commonly with intraclast mudstone breccias. Fine-grained packages are 1.2-3.5 m thick and 5-25 m width	Channel form (concave-up erosional basal bounding surface)	Fill or partial fill of abandoned channel segment
Overbank elements (4th order)		
(CR) Small-scale channnel. Apparent width: 2–15 m. Thickness: 0.4–1 m. Constituent lithofacies: Gm, St, Sla, Sr and Sl. Fining-upward trend.	Ribbon geometry and sharp top surface. Sometimes contains low-angle lateral-accretion surfaces.	Crevasse channel
(CS) Trough, ripple, and laminated assemblages (St, Sr, Fl) with a fining-upward grainsize trend. They are 0.5-1.0 m thick and can reach a maximum of 130 m of apparent width. Common mottling and *Skolithos* fossil traces.	Tabular unit, could show plane base and convex top	Crevasse-splay deposit
(LV) Rarely preserved. Interbedded St, Sr and Sm beds with fine-grained components (OF). Commonly associated with CS and CH elements.	Sheet-like to lenticular bodies 30-70 m long and 1-5 m thick, thinning away from a channel margin.	Levee.
(OF) Mudstone blankets, massive (Fm, Tm) or laminated (Fl, Tl), with or without minor sandstone lenses and/or sandstone load structures. Ocassional fine-ash strata (Tv) tens of cms. thick	Tabular unit	Suspension settling from unconfined flows during repeated minor flood events

Table II. Architectural elements of the Bajo Barreal Formation in Cerro Ballena anticline.

Fluvial styles

Five architectural styles have been identified for channel-belts, and two channel-belt-complex styles.

Alluvial architecture style 1: Multistorey, sheet-like channel belts dominated by downstream accretion. They represent 90% of sandbodies in the Cerro Ballena anticline. Basal contacts are sharp and ondulatory surfaces; lateral sandstone-body margins are either slightly incised wedge-shaped pinchouts onto fine-grained components, or vertically incised into previously deposited sediments. Multistorey sandbodies consist of a stack of multistory sandstone ribbons and sheets composed predominantly of downstream accreting (DA-CDA elements) barforms and tabular units of sandy materials (SB element), with abundance of laminated sandstones (SL element) toward the top. Single channel-fill deposits display isolated ribbon or sheet geometries, are up to 5.5 m thick and 20-350 m of true width; the larger deposits represent channel belts instead of single channels. Paleoflow data and dip accretion surfaces are roughly parallel (Fig. 3).

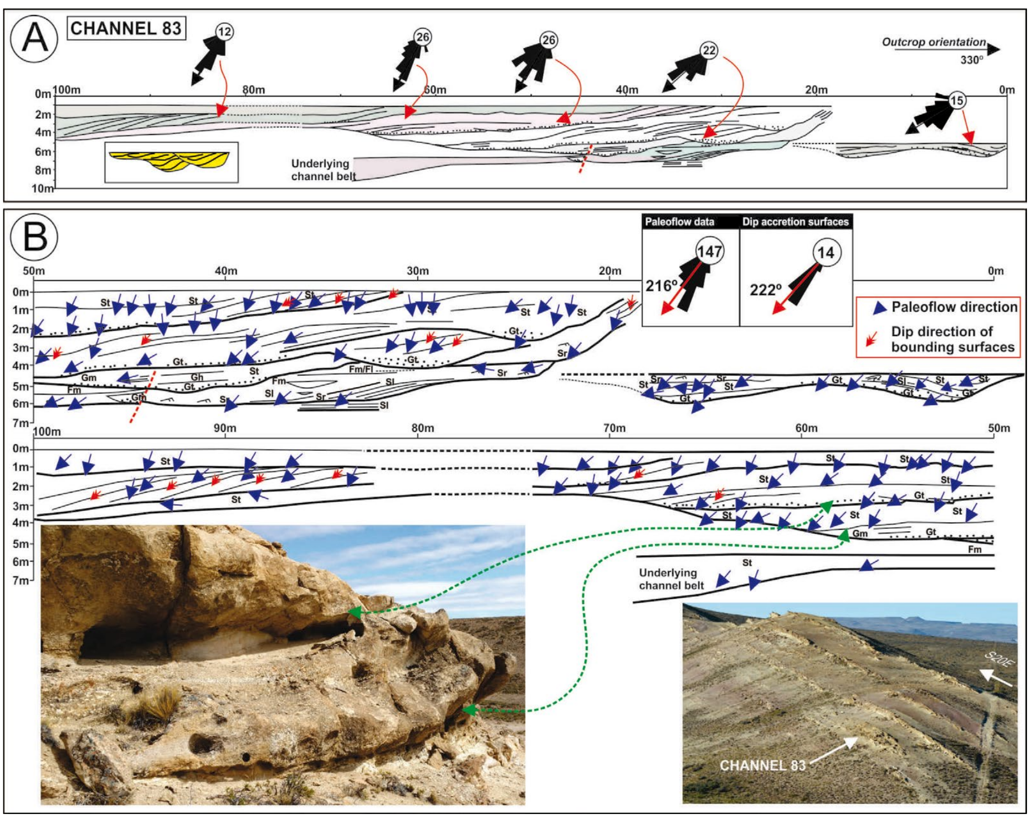

Figure 3. Fluvial architecture style 1: Multistorey, low-sinuosity channel belts dominated by downstream accretion. The upper panel (A) contains information of the main stories identified in the channel belt, with averaged paleocurrent values for each story. The inset shows a summary diagram with the main attributes. The lower panel (B) shows details of bedding characteristics, paleoflow data and dip accretion surfaces. For these vectors, the north is up to the page. Code of facies and architectural elements as in Tables I and II. Channel 83 belong to Section B, at the northernmost part of the study area.

Interpretation: The sheet-like external and internal geometry, overall low dispersion of paleocurrent direction, dominantly coarse-grained sediments, lack of evidence of lateral accretion, erosional bases and channelized nature of the infilling all indicate deposition within low-sinuosity alluvial channels. On the base of external and internal geometries, channels were up to 6 m depth, but typically 3-5 m, and sediment accumulated by the lateral shifting of channel across a broad channel belt. Preservation of massive siltstones below of erosional surfaces in multistorey sandbodies reflects abandonment and succesive relocation after avulsion. Most of DA elements are bars attached to a channel margin, with few examples of mid-channel bars of a braided river. From this, we consider that majority of the channels are integrated by alternate bar complexes along the channel margin and associated to a low-sinuosity thalweg (Miall 1996).

Alluvial architecture style 2: Multilateral, sheet-like channel belts dominated by downstream accretion. This type of channel belt has been identified in two (2) channel belts of Section B, and consists of couplets of: i) subordinate, erosionally based, sandy downstream-accretion large-scale strata (DA-CDA elements), that upward grade with ii) fine-grained sandstone wedges consisting of centimeter-scale ripple laminated and horizontally laminated siltstones. Channels were relatively narrow (30-45 m of width and 2.5-3.5 m thick) compared to channel-belt widths, with depths that correspond to the full height of the channel belt (~3.5 m). Paleoflow data and dip accretion surfaces are roughly parallel (Fig. 4).

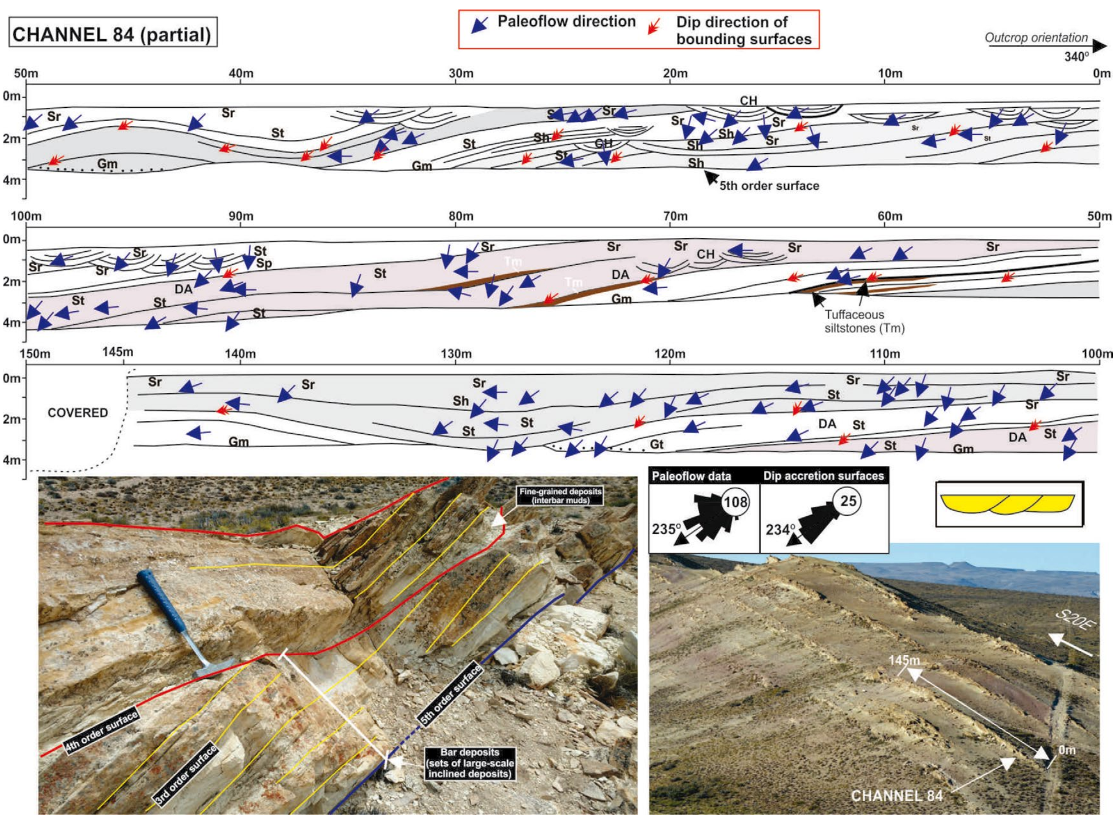

Figure 4. Fluvial architecture style 2: Multilateral, low-sinuosity channel belt dominated by downstream accretion. Section B, northernmost part of the study area. Abundance of DA elements is evidenced by the comparable direction of dip accretion surfaces and paleoflow data obtained from cross-bedding. Code of facies and architectural elements as in Tables I and II.

Interpretation: The dip direction for downstream accretion macroforms and paleoflow data of the stories indicate bar deposits in a low-sinuosity stream with predominance of sandy bedload, whereas the upper part of the stories reflects low-energy depositional conditions that could either represent the last stages of the river's existence before abandonment or a long-lasting, low-energy channel belt in a marginal position of a larger-scale channel belt. Channel fill elements indicate small and narrow channels, but the resulting channel belt can reach up to 630 m of true width and about 4.5 m of maximum thickness, evidencing lateral coalescense of stories with a multilateral arrangement (Potter 1967; Gibling 2006). The lateral mobility of these river systems had resulted in relatively high W/T values, in the range of broad sheets.

Alluvial architecture style 3: Sheet-like channel belts dominated by lateral accretion. This style

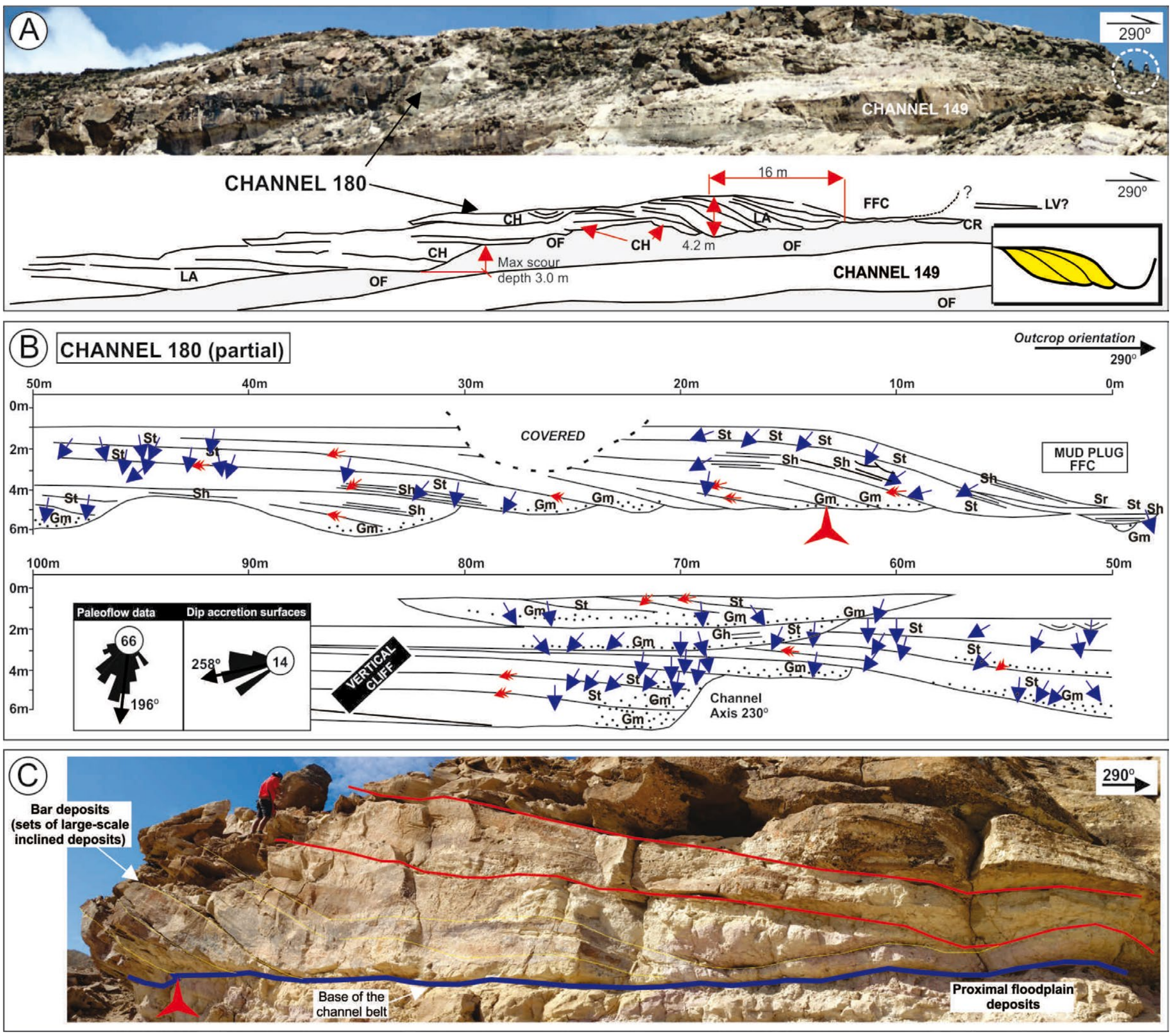

Figure 5. Fluvial Architecture style 3: Sheet-like channel belts dominated by lateral accretion. (A) Original photomosaic (Channel 180) and photo interpretation. Note lateral accretion stacking of the upper stories in the NNW channel belt margin, making up the main thickness of the channel-belt. (B) Line-drawing and facies of part of the meandering channel belt (Channel 180). Abundance of LA elements is evidenced by the high angle between the direction of dip accretion surfaces and paleoflow data on cross-bedding (inset). Code of facies and architectural elements as in Tables I and II. (C) Field example of lateral accretion bar deposits (bedsets). Colored lines are surfaces, with thicker lines indicating more significant surfaces.

is characterized either by sandstone channel belts consisting of several lateral stories with internal truncations and flat top, or by narrow abandoned channels on the top of the channel belt, then filled with tuffaceous mudstones. All the examples of this style (n=11) occur in Section B. The record of bedsets contain a basal coarse-grained channel lag (facies Gm) overlying a shallow (< 50 cm) scour, and are mainly made up of sediment deposited by plane bed (facies Sl) and migrating dunes (St and Sla facies), with interbedded rippled sandstones (facies Sr) and plane-parallel fine-grained sandstones (facies Sl) on top of the lensoidal bar-accretion set (Fig. 5). Identified bedsets range in thickness from 2.5-4.2 m, while the lenght of single point bars (measured from the shallow part of the channel toward the coarse-grained basal lag) range from 16-40 m of apparent width.

Interpretation: This channel-belt architecture reflects deposition by relatively large, stable, sinuous mixed-load rivers that deposited sand in point bars and tuffaceous mudstones locally in abandoned channels. The paleoflow depth of meandering rivers is the relief of fully preserved bar clinoforms (Allen 1965; Mohrig *et al.* 2000). While there may be some slight adjustment for compaction, the measurement of relief on fully preserved sigmoidal bar accretion sets should be close to true local flow depth. Thus, the channel in Fig. 5 has had a local flow depth up to 4.2 m.

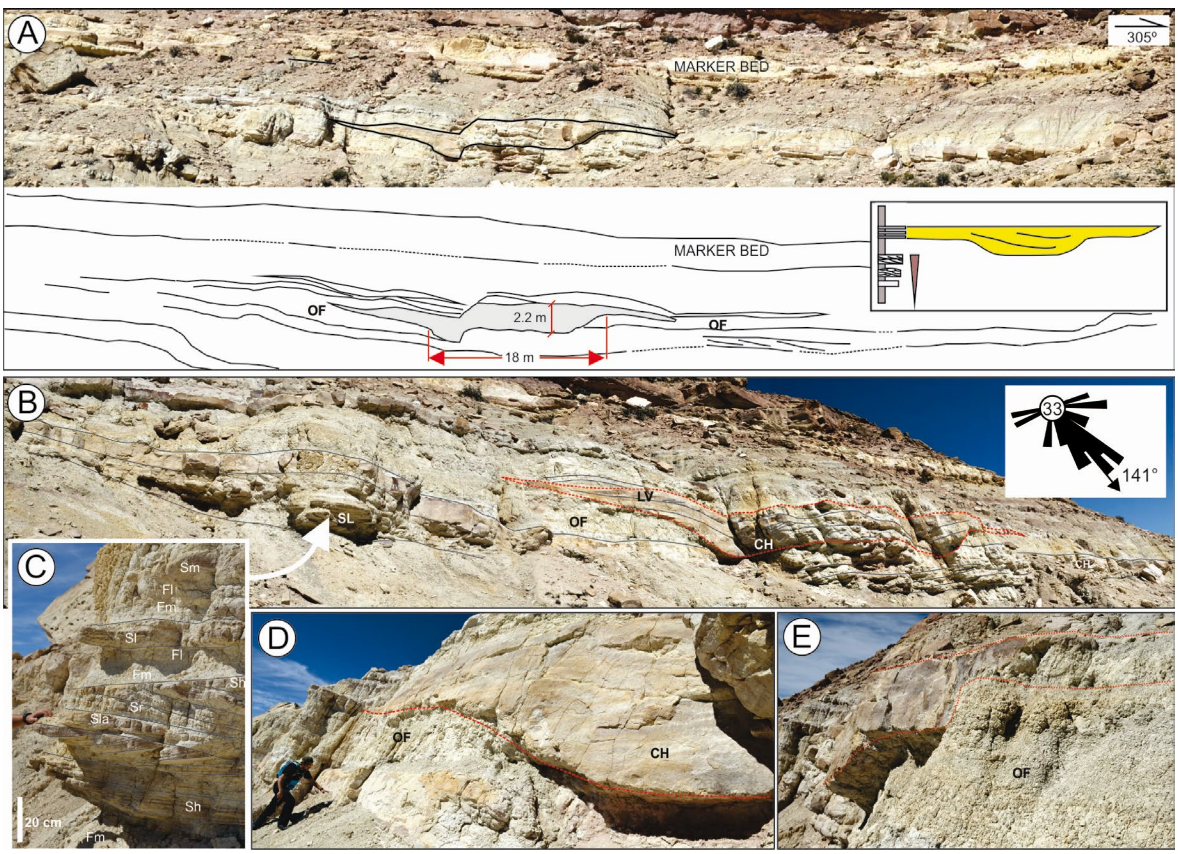

Figure 6. Fluvial architecture style 4: Channel belts containing ribbon-shaped single channels with attached splays. (A) Original photomosaic, photo-interpretation overlaid on photomosaic, and simplified sketch (inset). (B) Detailed bedding and architectural elements. Code of facies and architectural elements as in Tables I and II. (C) Facies arrangement of proximal floodplain deposits (Element SL y CR) underlying the selected channel belt. (D-E) Views of the basal scour of the ribbon channel.

Alluvial architecture style 4: Channel belts containing ribbon-shaped fixed channels with attached splays. Type 4 channel belts are not common but occur, with visible attached splays in Section A, representing ~ 1% of the analyzed channels. These sandbodies are almost symmetrical in cross section, with attached splays on both sides of the main channel fill (Fig. 6). The base of the channel is defined by a broadly symmetrical scour, cut into sheet siltstones and extending up to the points of splay attachment on either side. Paleoflow data from cross bedding (St) occurs towards the thalweg, with paleocurrents oriented into the outcrop. When identified, bar migration is roughly parallel to the paleoflow (DA element).

Interpretation: Single-story narrow and broad ribbon sandstone bodies (Gibling 2006) are interpreted as the deposits of low-sinuosity, fixed channels that produced DA elements during discharge events, intimately associated with the floodplain deposits within which they are encased. Overbank flooding during higher-magnitude discharge events produced splays attached to the CH elements forming a levee (LV element).

Aluvial architecture style 5: Ribbon or sheet-like channel belts dominated by resedimented volcaniclastics. This style of deposition is found in five channel belts, including the distinctive pale-grey to white marker bed located near the base of Section B (Fig. 7). In the marker bed, the volcaniclastic succession starts with a 0.7-1 m thick ash-dominated vitric tuff (Tm and Tl facies) identified along the entire western flank of the anticline. Overlying the vitric tuff, the strata shows planar base and consists of a 0.3 m thick package of coarse to medium-grained plane-laminated sandstone (Sl) containing isolated pebble clasts and inverse grading, followed upward by a 3-4 m thick, matrix supported, largely disorganized tuffaceous conglomerate (Gmv facies) in tabular bodies. Conglomerates are predominantly composed of pebble-sized, sub-angular tuffaceous or pumice components with a maximum clast size of 10 cm (mean around 2 cm) suspended in an ash-dominated, poorly sorted (cineritic to sandy) matrix, with variable content of sub-angular lithic fragments (< 2cm in size). Toward the top of the marker bed, sandy volcaniclastic strata containing horizontal bedding (Sl) and fining-upward trend is preserved. The most examples of channel belts of this style are thick channels (between 5.2 and 6.4 m of thickness) characterized by massive sandstones (Sm facies), minor Sl facies and rare diffuse St facies, with Gm facies overlying an erosive base.

Interpretation: This style of architecture is associated to channels that were occupied by debris flows and hyperconcentrated flood flows associated to intense rain events during periods of distal volcanic activity. The massive, matrix supported conglomerate (Gmv) and associated facies are either interpreted as debris flow or volcanic mudflows infilling shallow channels, both procceses associated to the cold reworking of volcanic particles by water. Volcanic mudflows contain at least 50% of sand, silt and mud as matrix, while volcanic debris flow contain up to 50% of coarse-grained particle concentration. Poor sorting, lack of low flow-regime sedimentary structures, presence of matrix-supported fabric and comparatively thick beds are all characteristics of subaerial mudflows/debris flows documented from both ancient and modern environments (Nemec and Steel 1984; Smith and Lowe 1991; Thouret and Lavigne 2000). Diffuse horizontal laminations at base and toward the top could be due to hyperconcentrated flood flows (Smith 1986; Sohn *et al.* 1999) in rapidly aggrading conditions. The remaining thick, ribbon channel belts of Section B (see Fig. 8) represent trunk channel systems that delivered large quantities of loose volcaniclastic material to the floodplain during floods.

Figure 7: Fluvial Architecture style 5. Channel belts dominated by resedimented volcaniclastics. Tuffaceous marker bed at base of Section B (sensu Figari *et al.* 1998). A fine-grained vitreous tuff at base (Facies Tvl, star) is covered by a 4,2 m thick, poorly organized tuffaceous conglomerate (Facies Gmm).

Alluvial architectural style 6: Unconfined, isolated sheet complex. This architectural style consists of multistorey, downstream accretion dominated channel belts of styles 1, 3, 4 and 5 with broad ribbon or narrow sheet geometry (Gibling 2006), surrounded by fine-grained (siliciclastic mudstone and siltstone) deposits. Poorly amalgamated to isolated channel belts are typical of Section A (see Fig. 8). Limited physical connectivity with other channel belts reflects the development of channel belts on wide floodplains.

Interpretation: The large vertical spacing and small width of channel belts in Section A is interpreted to be iether the product of higher subsidence rate or increased floodplain aggradation rate in relation to in-channel aggradation, which gave few opportunities for rivers to migrate and expand for a greater period of time before avulsion.

Alluvial architecture style 7: Unconfined, moderately amalgamated sheet complex. This style of alluvial architecture occurs in Section B and it is characterized by the development of partially connected multistorey sandstone broad ribbons and narrow sheets composed predominantly of downstream-accreting barforms but with some lateral accretion (Styles 1, 2 and 3). Channel belts in the cluster (Fig. 8) contain multiple internal scours, and the uppermost channel belt could contain a concave-up surface filled with a mud plug (as shown in Fig. 5). There is a large lateral variation in geometries (width, thickness) of the channels in the cluster, but the complex is dominated by downstream accretion, indicating a low-sinuosity river system. Although scarce, some sandbodies in the complex has overbank mudstone deposits lateral to the channel-belt margin, indicating that the channel belt was not confined within a valley. Lateral occurrence of channels with different sizes and planform shapes suggest the occurrence of coeval rivers that carried very different discharges, features shared in anastomosed (Makaske 2001) or anabranching river systems (North *et al.* 2007).

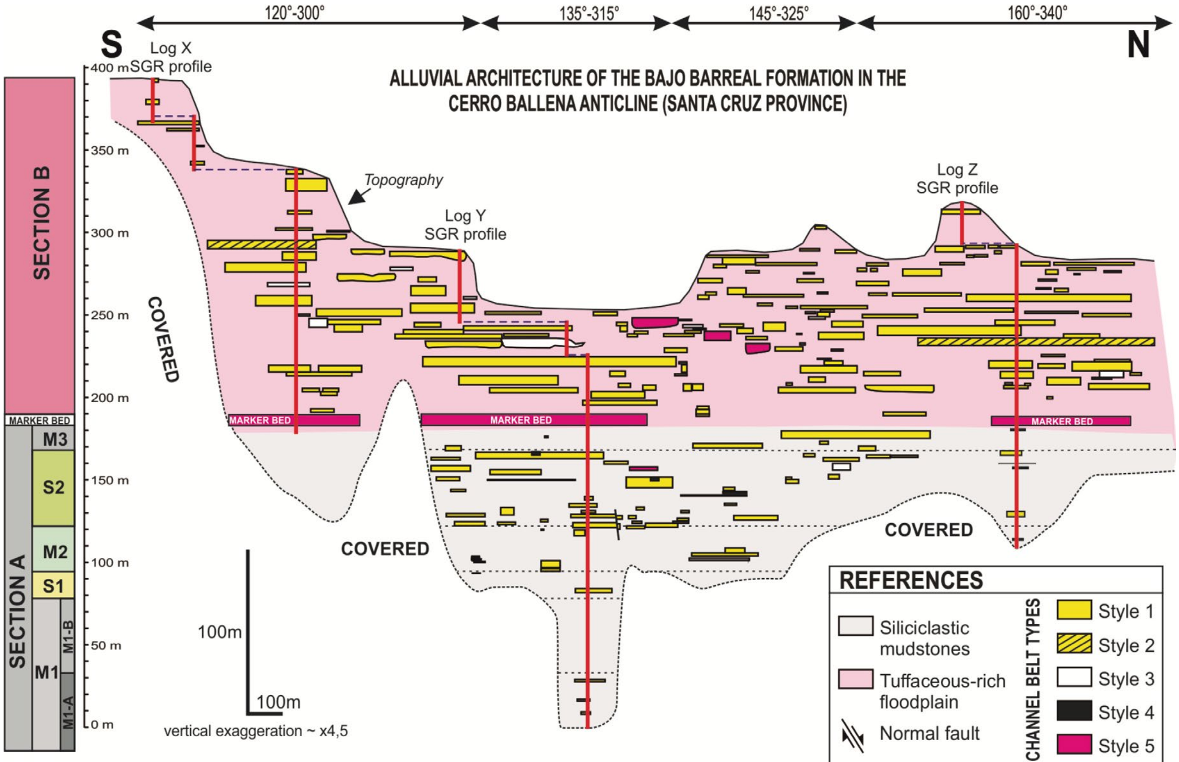

Figure 8. Panel showing mapped stratigraphy and facies architecture in the Bajo Barreal Formation along the western flank of the Cerro Ballena anticline. The represented width of channel belts is the apparent width. Major subdivisions of the SGR logs of Section A are present (see Paredes *et al.* this congress). Channel belts from Section A are mainly isolated (Alluvial architecture style 6) and of small scale, whereas channel belts of Section B are of larger scale and have moderately high connectivity (Alluvial architecture style 7).

Channel deposits: quantitative results

In this section, we summarize the measurements of the external geometry of single and multi-storey channels. Data are presented as graphs depicting the relationship between width and thickness, and can be used to predict sandstone-body width when only thickness (obtained from well log, core or measured section) information is available. Additionally, lateral/vertical variations in the net-to-gross ratio and a summary of paleoflow data are given.

Paleoflow measurements. A total of 3777 paleocurrent measurements have been carried out for the whole study, which allows defining 218 mean paleoflow vectors (Fig. 9A). The average paleoflow direction using the entire set of data is unimodal toward 187° (StD=45°), while the distribution of mean paleoflow vectors of channels show a bimodal distribution, with a main vector pointing SSW (185-200°), and a secondary mode toward SE (~140-150°). The classified rose of mean paleoflow vectors (Fig. 9B) shows that the main contribution to the mode is associated with sandbodies included in Section B. The rose diagram with radius proportional to maximum thickness (Fig. 9C) amplify the secondary mode toward SE (~150°), which is associated to channels up to 4 m thick. Moreover, thickness-weighted rose shows low paleoflow dispersion of the channel belts, rarely with paleoflow vectors toward NE. Some of those rare channels that flowed NE presumably were the source of published paleoflow data (Bridge *et al.* 2000, their Fig. 6), but still there is a large difference between the mean paleoflow vectors of this study (187°) and those indicated by Bridge *et al.* (2000), where a mean vector of 82° was reported.

The paleoflow distribution toward the SSW Az=187 , n=3777) is consistent with the occurrence of a southward depocenter, likely associated to a pre-Cretaceous extensional fault located south of the current course of the Deseado river. Paleoflow vectors toward NNE, NNW and NE identified adjacent to channels flowing SSW reflect both channel sinuosity (as indicated by curved meanders) or avulsion directions onto a virtually flat geomorphic scenario (see below).

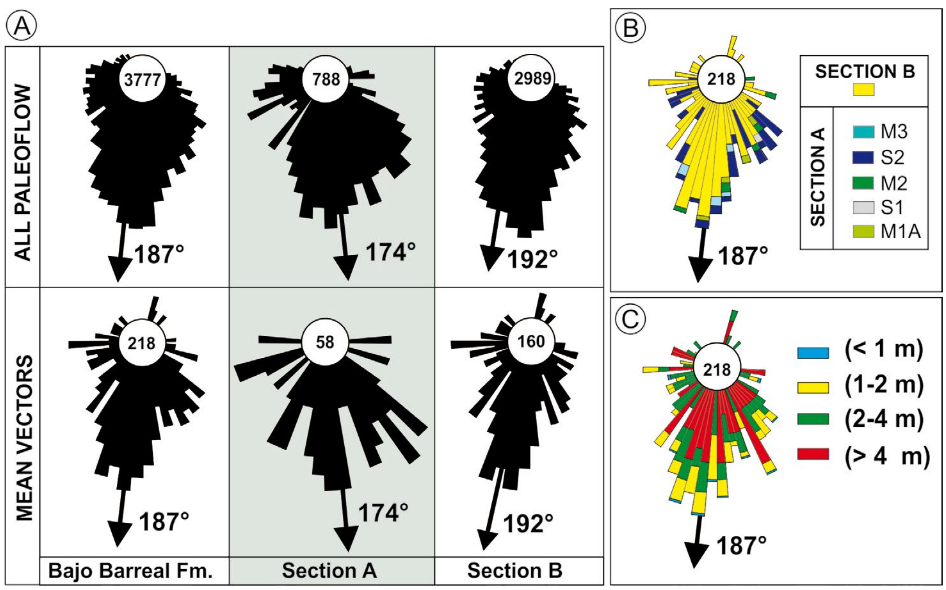

Figure 9. (A) Rose diagrams summarizing paleocurrent data of the Bajo Barreal Formation in the Cerro Ballena anticline, with distinction of data obtained in channel belts within the Sections A and B. Data using the mean vector of the channels reflect transportation toward SW-SE, subordinate transport toward W-WNW and rare data toward NE. (B) Rose diagram of mean paleoflow vectors classified according to its stratigraphic position. (C) Rose diagram of mean paleoflow vectors weighted according to its maximum thickness.

True width (W): For the entire dataset, true width (W) of channel deposits range from 2.8 m to 629.7 m, with a mean W of 57.5 m, while apparent width of sandbodies ranges from 8 m to 771 m with a mean W of 97.9 m. Mean apparent width obtained by Bridge *et al.* (2000) is razonably close to the data of the present dataset (112.87 m). The mean true width of sandbodies within Section

A is 45.7 m, reaching a maximum value of 177 m (Fig. 10A), whereas channels from Section B show a mean true width of 61.1 m and a maximum value of 629.7 m. The vertical distribution of geometries within Section A shows an increase of true width (W) throughout the unit (Fig. 10E). Channels within the M1 sub-unit have an averaged mean W of 18.8 m, while channels within M3 sub-unit show an averaged true width (W) of 68.7 meters. The mean of channels width of M3 sub-unit is quite similar to the mean width of section B (W mean = 61.6 m).

Maximum thickness (T): Maximum thickness of all sandbodies range from 0.4 m to 8.7 m, with a mean T of 2.5 m. Channels within the Section A show a general upward increase in T from sub-unit M1 (T mean=1.3 m) to sub-unit M3 (T mean=2.7 m) (Fig. 10E). The mean thickness of M3 is quite similar to the mean T of channelized sandbodies within Section B (2.6 m). The

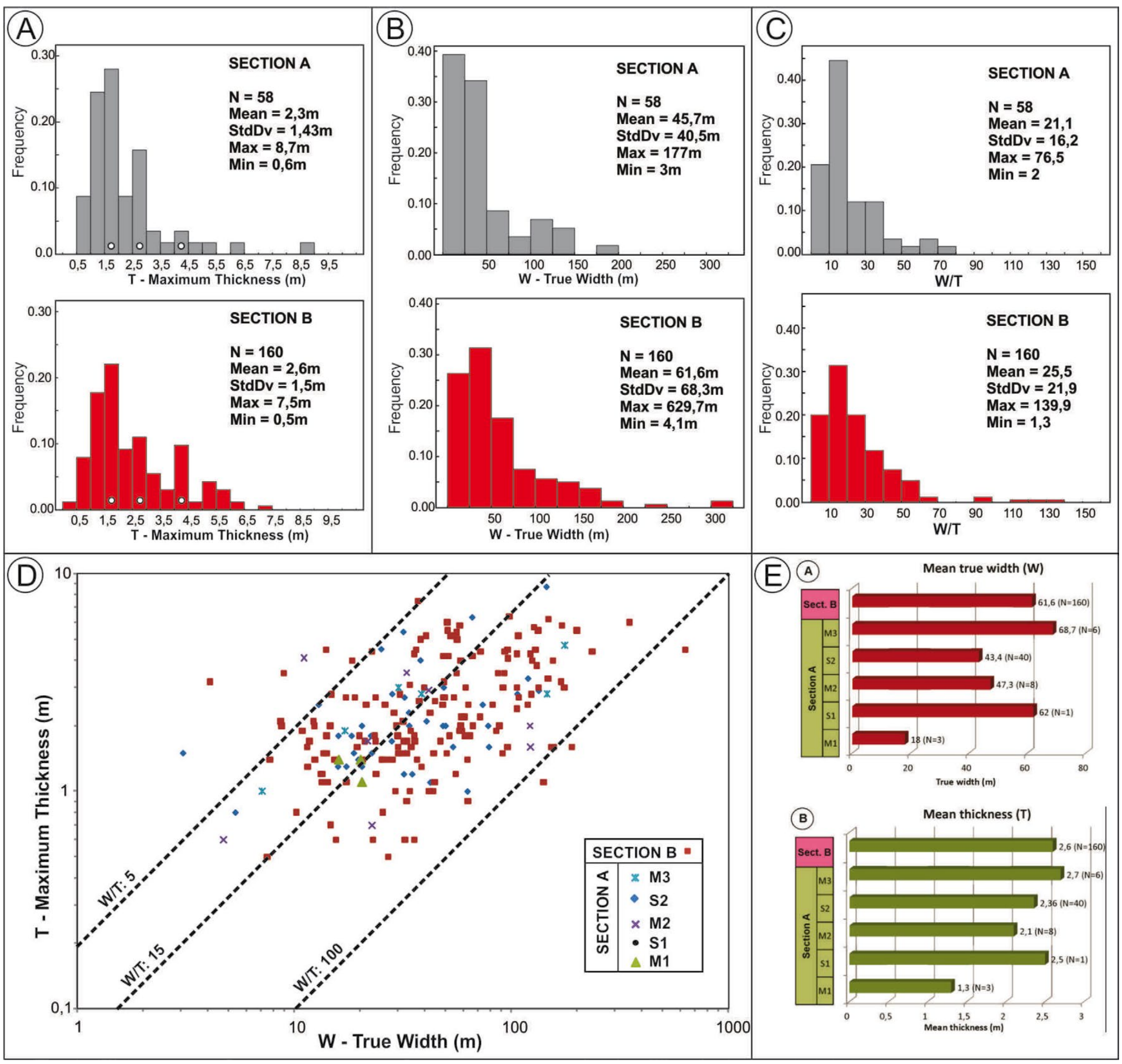

Figure 10. Comparative histograms of (A) maximum thickness, (B) true width, and (C) width:thickness ratio from channellized sandbodies of Sections A and B of the Bajo Barreal Formation in the Cerro Ballena anticline. A multilateral channel belt of 629 m of true width is not represented in (B). (D) W/T ratio of fluvial sandbodies of the Bajo Barreal Formation in Cerro Ballena anticline. (E) Vertical (temporal) variations in W and T of fluvial sandbodies in Bajo Barreal Formation at Ballena Hill. Note the vertical increase of T along Section A and the comparable external geometry of channels between the M3 sub-unit and Section B.

comparison of frequency histograms of channels between Sections A and B reveal high percentage of observations in the same interval of thickness (white circles in Fig. 10B), likely evidencing a hierarchical organization of large trunk channels and minor-scale tributaries in the fluvial system. Furthermore, Section B contains a second mode in the histogram around 5.5 m of thickness (12 sandbodies), representing the scale of the main trunk channels of the involved fluvial system.

Width/Thickness ratio (W/T): Sandbodies are mainly narrow sheets or broad ribbons that have an averaged W/T ratio of 24.4, with minor differences between Section A (W/T=21.1) and Section B (W/T=25.5) (Fig. 10C). As mentioned, both W and T of sandbodies of Section A gradually increase from sub-unit M1 to sub-unit M3, a trend only modified in sub-unit S1, which contain a single, large-scale sandbody that depart from the vertical trend of sizes (Fig. 10E). With this single exception, channels of Section A display a widening and thickening upward trend. The W/T crossplot (Fig. 10D) reflect channels with variable shape and scale flowing in the study area during deposition of each of the sub-units of Section A, and within Section B, implying variable discharge of the involved rivers. A likely fluvial system with main (trunk) rivers and tributaries of different scale is envisaged from the distribution of scales and geometries.

DISCUSSION AND CONCLUSIONS

A. Depositional model

The fluvial systems within the Section A (sensu Figari *et al.* 1998) are associated to perennial rivers and are multistorey, with ribbon or narrow sheet geometry, and dominated by downstream accretion of low-sinuosity channels, with rare fixed channels. Proximal floodplain deposits are commonly preserved below and in the margins of channel belts. The lack of distinctive levels containing mature paleosols suggests that movility of the channels was relatively high or that aggradation of the floodplain was high. The channel belts are physically isolated evidencing very-low connectivity, and separated from overlying channel belts by several meters to tens of meters of overbank fines, suggesting high rates in accommodation creation in relation to sediment supply (high A/S ratio, cf. Martinsen *et al.* 1999). The wide variety of channel sizes in Section A suggest the presence of rivers that carried very different discharges, where the largest channels are inferred to be deposits of major trunk rivers, whereas smaller channels of variable size and planview geometry are inferred to be tributaries or floodplain drainage channels in a multichannelized system (Fig. 11). The main mechanism of migration of channels and channel belts of Section A is considered autigenic avulsion produced by either progradation of channel belts onto previously deposited proximal floodplain deposits or by rapid relocation of the channel belt covering distal floodplain deposits. The dispersal pattern shows a consistent SSW-SSE paleoflow direction and reflect the location of a depocenter southward of the study area. Current classifications for multichannel fluvial systems that show variations of styles and geometries of the involved channels across the channel belts are commonly referred to some type of anabranching style (Nanson and Knighton 1996) but can also be referred to contra-style, plural sedimentation systems (sensu Lewin and Ashworth 2014). Paleoflow variations between adjacent or succesive channel belts along the unit resemble paleoflow distributions observed in both anastomosed fluvial systems (Stouthamer and Berendsen, 2001, 2007; Makaske *et al.* 2002, 2007) and anabranching fluvial systems (North *et al.* 2007).

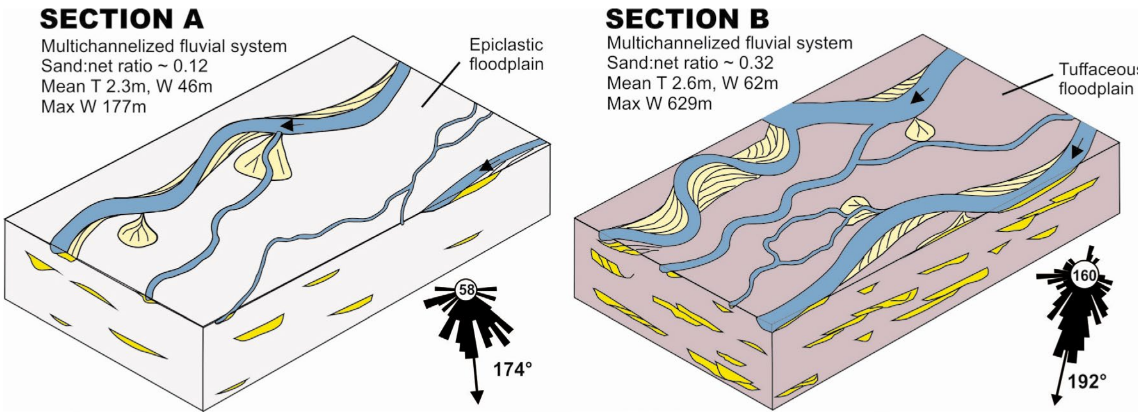

Figure 11: Conceptual model summarizing the alluvial architecture for the Section A and Section B of the Bajo Barreal Formation at Cerro Ballena anticline.

The fluvial systems of Section B are characterized by the occurrence of sheet-like channel fills with high interconnectivity, encased in a tuffaceus floodplain. Channels belts are mainly multistory packages dominated by downstream accretion, although meandering rivers are frequent. As in Section A, there is a large variation in thickness, width and external geometry of the sandbodies, reflecting variable discharge of the involved rivers; larger proportion of conglomerate facies in channelized facies of Section B also evidence flows of higher energy. Amalgamated channel-belt clusters of large channels along particular stratigraphic intervals of Section B are interpreted to record periods of lower accumulation rate relative to avulsion rate of the trunk river (Bridge and Leeder 1979; Shanley and McCabe 1994) and can be considered a low-accommodation system tract characterized by elevated connectivity of channel belts (Martinsen *et al.* 1999). Most of the analyzed fluvial channels relocated in the floodplain by avulsional processes (see below). Paleoflow during deposition of Section B evidence the continuity of the SSW paleotransport direction (Fig. 9). The increasing of the scale of sandbodies and coarser grain size of channels of Section B likely suggest a climatic shift toward more humid and wetter conditions upward.

B. Migracion styles

Detailed channel belt internal architecture (Architectural styles 1-5) and two different styles of stacking of channel belts complexes (Architectural styles 6-7) provide information of channel belt migration processes and mechanisms of re-occupation. We have found a low proportion of channel belt containing lateral accretion surfaces of meandering rivers (Architectural style 3, about 5% of the analyzed channel belts) or fixed channels in the floodplain (Architectural style 4, ~ 1%). The multilateral behavior of the channel belts (Architectural styles 2, < 1%) is also rarely established, and resedimentation of pyroclastic particles in sheet-like channel belts is uncommon (Architectural style 5, < 3%). From this, most of the channel belts reflect donwstream accretion of multistorey, low sinuosity channels, evidencing repeated re-occupation of channel depressions, likely associated to avulsion mechanisms in an anastomosed river system.

Three styles of avulsion have been previously documented: avulsion by channel reoccupation (avulsion by annexation sensu Slingerland and Smith 2004), avulsion by incision, and avulsion by progradation (Mohrig *et al.* 2000). Processes of sedimentation, water dispersal and the distribution and density of channels govern the three styles of avulsion (Jones and Hajek 2007). From our field review, we interpreted the three styles of avulsion, according to the criteria outlined below.

1) Avulsion by annexation: The channelized fluvial sandbodies (element CH) exhibit vertically amalgamated stories (Fig. 6B) that imply repeated reoccupation of the same site by avulsing channels (Aslan and Blum 1999; Mohrig *et al.* 2000). Lenses of fine-grained floodplain deposits situated towards the top and within multistorey channel belts provide evidence for channel abandonment in relative lows on the floodplain, prior to reoccupation following a later avulsion. Multistory sandbodies may cut down into CS/LV (<1.5 m thick) or OF element. These architectures are interpreted to record avulsion by annexation, whereby flow-path selection takes place via channel re-localization. Avulsion by progradation or incision may lead to avulsion by re-occupation when the progradation of crevasse splays or levees redirect new avulsion channels towards a previous site of avulsion (Singerland and Smith 2004).

2) Avulsion by progradation. Some channelized sandbodies consists of either single-story, isolated or multistory packages that cut into a subjacent succession of upward-thickening or upward-thinning crevasse splay beds (Elements CR, CS/LV). The thickness of strata cropping out beneath the channel belt ranges between 2.5 to 8 m. The splay deposits contain weakly developed paleosols and mottled fine-grained materials interbedded with fine to medium-grained sandstones. This alluvial organization is interpreted to record progressive increases in sedimentation rate and gradual progradation of a fluvial channel into a topographically low part of a floodplain preceding avulsion ("stratigraphically transicional avulsion" sensu Jones and Hajek 2007). Where an isolated channelized fluvial sandbody story cuts into a subjacent succesion of upward-thinning crevasse splay beds (examples in Fig. 2), this may represent a decrease in proximity to a fluvial channel prior to avulsion. However, the underlying crevasse-splay complex may still be genetically related to the overlying channelized fluvial sandbodie story, since crevasse-splay complexes exhibit much lateral variation in geometries at bed scale (Smith *et al.* 1989; Fisher *et al.* 2007), directly linked to the micro-topography of the floodplain. Both of these architectures are interpreted to record avulsion by progradation and involve a phase of deposition prior to avulsion (Slingerland and Smith 2004).

3) Incisional avulsion: In this style of avulsion the channelized fluvial sandbodies consists of stories that cut directly into subjacent fine-grained floodplain deposits (Element OF), without preservation of CR, CS or LV element (several examples in Fig. 2). This architecture is interpreted to record the abrupt introduction of a fluvial channel by avulsion and record avulsion by incision (Singerland and Smith 2004). This style of avulsion indicates a period of nondeposition prior to avulsion, and sudden avulsion to areas of the floodplain that were subject to slow gradual sediment accumulation (Jones and Hajek 2007). Incisional avulsion has been considered as the dominant avulsion mechanism in the analyzed exposures of the Bajo Barreal formation, also identified as the main mechanism in other exposures of the unit (Paredes *et al.* 2016) and in the overlying Lago Colué Huapi formation (Casal *et al.* 2015).

C. Implications for subsurface studies

The results of this study allow elucidation of several problems facing subsurface characterization of fluvial reservoirs in the Bajo Barreal Formation, as follow:

a) Outcrop analogs can be used to make predictions of the true channel width of potential reservoirs in nearby oilfields. Our database of width, thickness and W/T based in measurements on 218 channels provides a basis for quantitative use of channel thickness derived from well logs and/or cores, in order to make estimations of true width of channel/channel belts in the subsurface. Although variable, the results indicate wider channels occur in parallel with thicker channels.

b) The field study provides a relation between channel size and channel connectivity. We have found that stratigraphic intervals with higher interconnectivity (Section B) contain channels of larger scale (width, thickness) than those of intervals of lower interconnectivity (Section A). As channel sizes are related to water availability and discharge of the formative rivers, it is suggested a climatic control on the channel interconnectivity (see also Paredes *et al.* this congress)

c) Subsurface fluvial models require characterization of channel patterns to make predictions of location and style of channel fills. Outcrop analogs in the Cerro Ballena anticline show a complex fluvial architecture with several architectural styles developed at coeval levels in a multichannel fluvial system. From this, simplistic (unrealistic) reservoir models characterized by a single channel pattern (eg. braided or meandering) should be seen with due care.

d) The study provides a reliable outcrop analog to understand migration styles of fluvial channels in the subsurface. This study has found that some sandstone bodies have well developed lateral accretion surfaces and a meandering planform, but most of the channels migrated by incisional avulsion. In many examples of the subsurface of the Golfo San Jorge San Jorge basin, fluvial channels/channel belts (4-15 m thick) rest directly atop of fine-grained successions (several tens of meters thick) without coarsening upward or fining-upward log motifs (below or above of the channel belt, respectively). From this, we consider incisional avulsion as a major mechanism of migration of channel belts in the subsurface.

e) Additionally, the observed paleoflow distribution toward the SSW-SSE opens an unresolved question: Where the rivers have gone?

ACKNOWLEDGMENTS

We would like to thank SINOPEC ARGENTINA E&P for permission to publish the results. The authors are indebted to landowners of estancia Cañadon Vasco (family Bain) for access to outcrops. This research was partially supported by the Agencia Nacional de Promoción Científica y Tecnológica (PICT 2012-1369). The comments of two anonymous reviewers helped to improve the final quality of the final version.

REFERENCES

Allen, J.P., C.R. Fielding, M.R. Gibling and M.C. Rygel, 2014, Recognizing products of palaeoclimate fluctuations in the fluvial stratigraphic record: an example from the Pennsylvanian to Lower Permian of Cape Breton Island, Nova Scotia. Sedimentology, 61: 1332-1381.

Allen, J.R.L., 1965, Fining upward cycles in alluvial successions. Geological Journal, 4: 229-246.

Allen, J.R.L., 1983, Studies in fluviatile sedimentation: bars, bar-complexes and sandstone sheets (low-sinuosity braided streams) in the Brownstones (L. Devonian), Welsh borders: Sedimentary Geology, 33: 237-293.

Aslan, A. and M.D. Blum, 1999, Contrasting styles of Holocene avulsion, Texas Gulf Coastal Plain. In: Smith, N.D. and J.J. Rogers, (eds.), Current Research in Fluvial Sedimentology: International Association of Sedimentology, Special Publication 28: 193-209.

Bridge, J.S., 1993, The interaction between channel geometry, water flow, sediment transport and deposition in braided rivers. In: Best, J.L. and C.S. Bristow (eds.) Braided Rivers. Geological Society of London, Spec. Publ., 75: 13-71.

Bridge, J.S., 2003, Rivers and Floodplains: Forms, Processes and Sedimentary Record. Blackwell, p. 1-491.

Bridge, J.S. and M.R. Leeder, 1979, A simulation model of alluvial stratigraphy. Sedimentology, 26: 617-644.

Bridge, J.S., G.A. Jalfin and S.M. Georgieff, 2000, Geometry, lithofacies, and spatial distribution of Cretaceous fluvial sandstone bodies, San Jorge Basin, Argentina: outcrops analog for the hydrocarbon-bearing Chubut Group. Journal of Sedimentary Research, 70: 319-337.

Casal, G.A., J.O. Allard and N. Foix, 2015, Análisis estratigráfico y paleontológico del Cretácico superior en la cuenca del Golfo San Jorge: nueva unidad litoestratigráfica para el Grupo Chubut. Revista de la Asociación Geológica Argentina, 72: 81-99.

Di Benedetto, L., S.M Georgieff and G. Potas, 2006, Stratigraphic correlation and sedimentary analogs: Ballena Hill outcrops and Cañadón Vasco oil field, Southern flank of San Jorge Basin, Argentina. Simposio Bolivariano de Hidrocarburos, Cartagena de Indias, Colombia, 12 p.

El-Mowafy, H.Z. and K.J. Marfurt, 2016, Quantitative seismic geomorphology of the middle Frio fluvial system, south Texas, United States. American Association of Petroleum Geologists Bulletin, 100: 537-564.

Figari, E.G., S.F. Courtade, R. Calegari, H. Arroyo and L. Constantini, 1998, Estructura y estratigrafía del Cerro Ballena, Faja Plegada meridional de la Cuenca del Golfo San Jorge. X Congreso Latinoamericano de Geología and VI Congreso Nacional de Geología Económica, 1, 18-23. Buenos Aires.

Fisher, J.A., G.J. Nichols and D.A. Waltham, 2007, Unconfined flow deposits in distal sectors of fluvial distributary systems: Examples from the Miocene Luna and Huesca Systems, northern Spain. Sedimentary Geology, 195: 55-73.

Ghinassi, M., A. Iepi, M. Aldinucci and M. Fustic, 2016, Downstream-migrating fluvial point bars in the rock record. Sedimentary Geology, 334: 66-96.

Gibling M.R., 2006, Width and thickness of fluvial channel bodies and valley fills in the geological record: a literature compilation and classification. Journal of Sedimentary Research, 76: 731-770.

Hajek, E.A. and M.A. Wolinsky, 2012, Simplified process modeling of river avulsion and alluvial architecture: connecting models and field data. Sedimentary Geology, 257: 1-30.

Jones, H.J. and E.A. Hajek, 2007, Characterizing avulsion stratigraphy in ancient alluvial deposits: Sedimentary Geology, 202: 124-137.

Keogh, K.J., S. Leary, A.W. Martinius, A.S.J. Scott, S. Riordan, I. Viste, S. Gowland, A.M. Taylor and J. Howell, 2014, Data capture for multiscale modelling of the Lourinhã Formation, Lusitanian Basin, Portugal: an outcrop analogue for the Statfjord Group, Norwegian North Sea. In: Martinius, A.W., J.A. Howell and T.R. Good (eds.) Sediment-Body Geometry and Heterogeneity: Analogue Studies for Modelling the Subsurface. Geological Society, London, Special Publications, 387: 27-56.

Makaske, B., 2001, Anastomosing rivers: a review of their classification, origin and sedimentary products. Earth-Science Reviews, 53: 149-196.

Makaske, B., D.G. Smith and J.A. Berendsen, 2002, Avulsions, channel evolution and floodplain sedimentation rates of the anastomosing upper Columbia River, British Columbia, Canada. Sedimentology, 49: 1049-1071.

Makaske, B., J.A. Berendsen and M.H.M. van Ree, 2007, Middle Holocene avulsion-belt deposits in the Central Rhine–Meuse delta, The Netherlands. Journal of Sedimentary Research, 77: 110-123.

Martinsen, O., A. Ryseth, W.H. Hansen, H. Fleshe, G. Torkildsen and S. Idil, 1999, Stratigraphic base level and fluvial architecture: Ercson Sandstone (Campanian), Rock Springs Uplift, SW Wyoming, USA. Sedimentology, 46: 235-259.

Miall, A.D., 1985, Architectural-element analysis: a new method of facies analysis applied to fluvial deposits. Earth-Science Reviews, 22: 261-308.

Miall, A.D., 1996, The Geology of Fluvial Deposits. Springer, 582 p. Berlín.

Mohrig, D., P.L. Heller, C. Paola and W.J. Lyons, 2000, Interpreting avulsion process from ancient alluvial sequences: Guadalupe-Matarranya (Northern Spain) and Wasatch Formation (Western Colorado). Geological Society of America Bulletin, 112: 1787-1803.

Nemec, W. and R.J. Steel, 1984, Alluvial and coastal conglomerates: their significant features and some comments on gravelly massflow deposits. In: Koster, E.H. and R.J. Steel, (eds.) Sedimentology of gravels and conglomerates. Canadian Society of Petroleum Geologists, Memoir 10, p. 1-31.

North, C.P., G.C. Nanson and S.D. Fagan, 2007, Recognition of the sedimentary architecture of dryland anabranching (anastomosing) rivers: Journal of Sedimentary Research, 77: 925-938.

Paredes, J.M., N. Foix and J.O. Allard, 2016, Sedimentology and alluvial architecture of the Bajo Barreal Formation (Upper Cretaceous) in the Golfo San Jorge Basin: outcrop analogues of the richest oil-bearing fluvial succession in Argentina. Marine and Petroleum Geology, 72: 317-335.

Paredes, J.M., S.R. Giordano, M.N. Valle, J.O. Allard and N. Foix, this congress, Spectral gamma-ray logging of Cerro Ballena anticline, Santa Cruz province: an outcrop analogue to subsurface characterization and well-log correlation to fluvial sandstone reservoirs. 10º Congreso de Exploración y Desarrollo de Hidrocarburos, Mendoza.

Posamentier, H.W., R.J. Davies, J.A. Cartwright and L. Wood, 2007, Seismic geomorphology - an overview. In: Davies, R.J., H.W. Posamentier, L.J. Wood and J.A. Cartwright, (eds.) Seismic Geomorphology: Applications to Hydrocarbon Exploration and Production. Geological Society, London, Special Publication 277: p. 1-14.

Potter, P.E., 1967, Sand bodies and sedimentary environments: a review: American Association of Petroleum Geologists Bulletin, 51: 337-365.

Pranter, M.J., A.C. Hewlett, R.D. Cole, H. Wang and J. Gilman, 2014, Fluvial architecture and connectivity of the Williams Fork Formation: use of outcrop analogues for stratigraphic characterization and reservoir modelling. In: Martinius, A.W., J.A. Howell and T.R. Good, (eds.) Sediment-body geometry and heterogeneity: analogue studies for modelling the subsurface. Geological Society of London, Special Publication 387, p. 57-83.

Ramsay, J.G., 1961, The effects of folding upon the orientation of sedimentary structures. Journal of Geology, 69: 84-100.

Rittersbacher, A., S.J. Buckley, J.A. Howell, G.J. Hampson and J. Vallet, 2014. Helicopter-based laser scanning: a method for quantitative analysis of large-scale sedimentary architecture. In: Martinius, A.W., J.A. Howell and T.R. Good, (eds.) Sediment-body geometry and heterogeneity: analogue studies for modelling the subsurface. Geological Society of London, Special Publication 387: 185-202.

Secretaría de Energía, 2016. Informe estadístico anual 2016 del sector energético. Ministerio de Energía y Minería. Secretaría de Planeamiento Energético Estratégico, 40p.

Shanley, K.W. and P.J. McCabe, 1994, Perspectives on the sequence stratigraphy of continental strata. American Association of Petroleum Geologists Bulletin, 78: 544-568.

Smith, G.A., 1986, Coarse-grained nonmarine volcaniclastic sediment: Terminology and depositional processes. Geological Society of America Bulletin, 97: 1-10.

Smith, G.A. and D.R. Lowe, 1991. Lahars: volcano-hydrologic events and deposition in the debris flow-hyperconcentrated flow continuum. In: Fisher, R.V. and G.A. Smith (eds.), Sedimentation in Volcanic Settings. Society for Sedimentary Geology, Special Publication 45, p. 59-70. Tulsa.

Smith, N.D., T.A. Cross, J.P. Dufficy and S.R. Clough, 1989, Anatomy of an avulsion. Sedimentology, 36: 1-23.

Sohn, Y.K., C.W. Rhee and B.C. Kim, 1999, Debris flow and hyperconcentrated flood-flow deposits in an alluvial fan, northwestern part of the Cretaceous Yongdong basin, central Korea. Journal of Geology, 107: 111-132.

Stouthamer, E. and H.J.A. Berendsen, 2001, Avulsion frequency, avulsion duration, and interavulsion period of Holocene channel belts in the Rhine-Meuse Delta, the Netherlands. Journal of Sedimentary Research, 71: 589-598.

Stouthamer, E. and H.J.A. Berendsen, 2007. Avulsion: the relative roles of autogenic and allogenic processes: Sedimentary Geology, 198: 309-325.

Thouret J-C. and F. Lavigne, 2000, Lahars: occurrence, deposits and behaviour of volcano-hydrologic flows. In: Leyrit, H. and C. Montenat (eds.) Volcaniclastic rocks, from magmas to sediments. Gordon & Beach Science Publishers, p. 151-174.